Chemical Engineering Science 327 (2026) 123622

Contents lists available at ScienceDirect

Chemical Engineering Science

journal homepage: www.elsevier.com/locate/ces

Optimizing product yield and composition in chemical recycling of mixed plastics through temperature-staged pyrolysis

Niklas Netsch, Aljoscha Tauber, Daniela Merz, Britta Bergfeldt, Salar Tavakkol *, Dieter Stapf

Institute for Technical Chemistry, Karlsruhe Institute of Technology, Kaiserstraße 12, 76131 Karlsruhe, Germany

ARTICLE INFO

Keywords:
Chemical recycling
Mixed thermoplastics
Temperature-staged pyrolysis
Thermogravimetry
Stirred tank reactor
Process optimization

ABSTRACT

Chemical recycling of plastic waste via pyrolysis contributes to higher recycling rates in a circular economy. One important prerequisite is the conformity of pyrolysis products with defined chemical feedstock specifications. In the pyrolysis of mixed plastics, specification compliance is particularly hindered by the presence of aromatic compounds and heteroatom-containing species (e.g., Cl, N, O) in the pyrolysis oils. Temperature-staged pyrolysis facilitates oil decontamination, but scaling up this concept in pyrolysis processes poses challenges. Therefore, investigations in thermogravimetry (TG) and a scalable stirred-tank reactor (STR) system are performed. Under well-defined TG conditions, low temperature stages allow for dehalogenation and the selective decomposition of non-polyolefinic polymers. Polyolefins decompose mainly in a separate stage at higher temperatures above 400 °C. Polymer interaction effects significantly influence the decomposition kinetics and depend strongly on the polymer type in the mixture. The application in the STR system confirms technical feasibility, but also reveals scale-up engineering challenges through heat and mass transfer limitations. The heat transfer limitations reduce the polymer temperature during the two-staged STR process, requiring a higher first-stage set temperature than in TG. Compared to isothermal pyrolysis at 500 °C, the total heteroatom content in the oil produced in the second stage decreases. Toluene, benzoic acid, and ε-caprolactam content are reduced by a factor of 2–3 while aliphatic compounds are enriched. Staging also facilitates the separation of heteroatom-containing gases from the aliphatic-rich gas fraction. In contrast, elevating the first-stage pyrolysis temperature from 370 °C to 430 °C reduces the target product yield from 56 wt.% to 23 wt.%. However, the temperature elevation also results in a higher quality of the target product because of a reduced amount of incorporated non-aliphatic compounds. These findings highlight the trade-off between maximizing the yield and enhancing the quality of the aliphatic-rich target product fraction.

1. Introduction

The growing environmental burden of plastic waste and the need for efficient resource management have intensified research into improving the sustainability of plastic manufacturing and waste utilization (Keijer et al., 2019). Establishing a circular economy for plastic products appears to be key in this context (van Geem, 2023). To promote its progress, the European Union introduced strict recycling targets in 2021 (Parliament, 2018). At present, the mechanical recycling of most waste fractions is technically limited because of their heterogeneity and existing contaminations (Ragaert et al., 2017). Chemical recycling processes offer an approach to raise recycling rates for polymeric materials (Johansen et al., 2022). In particular, thermochemical processes such as pyrolysis and gasification are promising because of their feedstock flexibility and the product reintegration into various established chemical industry processes (Rahimi and García, 2017). While gasification aims to recycle via C_1-chemistry, pyrolysis allows substituting crude oil fractions or even direct monomer production for polymer synthesis at comparatively lower temperatures (Palos et al., 2019; Holtkamp et al., 2024).

Abbreviations: ABS, Acrylonitrile butadiene styrene; FID, Flame ionization detector; GC, Gas chromatography; GCxGC, Two-dimensional GC; HC, Hydrocarbon; HDPE, High-density polyethylene; LDPE, Low-density polyethylene; MS, Mass spectrometer; PA6, Polyamide 6; PET, Polyethylene terephthalate; PP, Polypropylene; PS, Polystyrene; PVC, Polyvinyl chloride; STR, Stirred tank reactor; TCD, Thermal conductivity detector; TG, Thermogravimetry.

* Corresponding author.
E-mail address: Salar.Tavakkol@kit.edu (S. Tavakkol).

https://doi.org/10.1016/j.ces.2026.123622
Received 24 November 2025; Received in revised form 10 February 2026; Accepted 13 February 2026
Available online 15 February 2026

In pyrolysis, product yields and composition strongly depend on the waste plastic feedstock (Laghezza et al., 2024). Thermoplastic polymers dominate the waste streams relevant for chemical recycling (Geyer et al., 2017). These are polyethylene (PE), polypropylene (PP), polystyrene (PS), polyethylene terephthalate (PET), polyamide (PA), and polyvinyl chloride (PVC). Each of these polymers forms different pyrolysis products, as their reaction mechanisms depend on the molecular structure of the plastic type (Bockhorn et al., 1999; Bockhorn et al., 1999; Faravelli et al., 2001; Montaudo et al., 1993; Yu et al., 2016; Lee et al., 2006).

Enabling chemical recycling requires converting pyrolysis products into base chemicals for polymer synthesis. This conversion is enabled by reintegrating the generated pyrolysis products in cracking plants of the chemical industry. For successful reintegration, they must meet fossil-based feedstock specifications (Palos et al., 2019; Kusenberg et al., 2022). Thus, such cracking plants represent the final gate in a waste-to-polymer or waste-to-chemicals recycling concept. Mixed waste streams, in particular, consist largely of PE and PP, which often results in the formation of aliphatic-rich pyrolysis products. Nevertheless, high dilution of pyrolysis oils with fossil-based feedstocks or upgrading are necessary, as heteroatom contaminations by oxygen-, nitrogen-, or chlorine-containing hydrocarbons (HC) reduce the pyrolysis product quality (Kusenberg et al., 2022). A high aromatic content in the pyrolysis oil also hinders its application (Kusenberg et al., 2022), except if the aromatic contents reach a level where direct monomer separation is beneficial (Holtkamp et al., 2024). Pyrolysis oils usually exhibit a high proportion of olefins, which hinders their reintegration (Kusenberg et al., 2022).

Different techniques for improving the pyrolysis oil quality have been reported in the literature. The use of catalysts (Laghezza et al., 2024; Zhang et al., 2024) or solid sorbents (Cao et al., 2025) can shift the product composition or remove chlorine-based contaminants. Downstream oil upgrading via hydrotreating, filtration, solvent extraction, and distillative fractionation offers a promising approach to obtain specification-compliant pyrolysis products suitable for reintegration (Kusenberg et al., 2022). Alternatively, thermochemical feedstock pretreatment, such as low-temperature torrefaction, improves the pyrolysis oil quality by reducing the heteroatom content in the pyrolyzed feedstock (Kumar et al., 2024). However, all of these strategies require additional reactors or separation systems, which increase investment costs and can introduce additional technical difficulties.

Yet the polymer-specific differences in the decomposition mechanism and, thus, the decomposition kinetics allow the direct, in-situ process optimization of plastic pyrolysis. In particular, thermoplastics that contain chlorine, oxygen, nitrogen, or aromatic groups in their polymeric structure decompose at lower temperatures than polyolefins (Netsch et al., 2025). Fig. 1 shows the temperature-dependent decomposition curves of the most commonly produced thermoplastics and the copolymer acrylonitrile butadiene styrene (ABS) (Netsch et al., 2026). The polymer-specific decomposition ranges are highlighted. PVC pyrolyzes according to a two-stage decomposition mechanism (Yu et al., 2016). In the first dehalogenation phase above approximately 230 °C, HCl is released, and polyene chains form (Yu et al., 2016). These polyene chains degrade slowly at elevated temperatures to form aromatic structures, unsaturated aliphatics, and 6.6 wt.% of coke (Yu et al., 2016; Netsch et al., 2025). All other thermoplastics each exhibit individual single-stage decomposition mechanisms, whereby the onset pyrolysis temperatures differ, and only PET exhibits relevant coke formation (Montaudo et al., 1993). Despite differing onset temperatures, the degradation ranges overlap, raising the need for more detailed investigation.

The concept of temperature-staged pyrolysis was already investigated for mixed plastics in the late 1990 s by Bockhorn et al., conducting experiments with defined mixtures of PE, PS, PA6, and PVC (Bockhorn et al., 1998; Bockhorn et al., 1999). The chlorine content could be significantly minimized in the target product by selective temperature staging. Furthermore, the temperature staging for model mixtures of

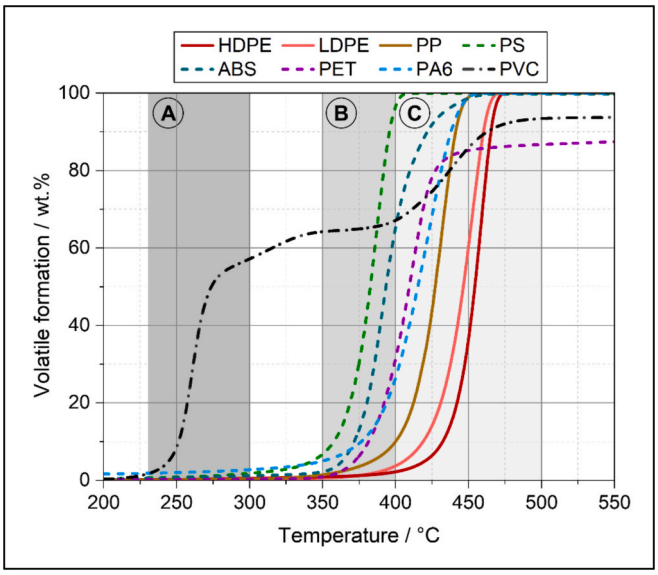

Fig. 1. TG experiments with different thermoplastics showing the main degradation ranges for PVC dehalogenation (A), PS, ABS, PET, and PA6 decomposition (B), and decomposition of polyolefins and PVC polyene chains (C) at a constant heating rate of 2 K/min (adapted from (Netsch et al., 2025).

PVC, PS, PA6, and PE allowed the generation of a styrene- and caprolactam-rich pyrolysis oil separate from an aliphatic condensate. The concept was then transferred to plastic waste from electronic equipment (Bockhorn et al., 1999). At the same time, Faravelli et al. proved the styrene monomer enrichment by staged pyrolysis with PE and PS mixture in TG experiments (Faravelli et al., 2003). Also, they performed kinetic modeling of stepwise pyrolysis.

Further investigations of this pyrolysis concept were conducted by other authors (Korkmaz et al., 2009; Cheung et al., 2011; Oyedun et al., 2013; Choi et al., 2016; Oyedun et al., 2012; Fukushima et al., 2010; López et al., 2011; Lopez-Urionabarrenechea et al., 2012; Yuan et al., 2014; Yin et al., 2021; Park et al., 2018; Park et al., 2019; Park et al., 2022; Sophonrat et al., 2018; Chang et al., 2023). Other feedstocks were tested, such as cellulose-based composite packaging (Korkmaz et al., 2009), scrap tires (Cheung et al., 2011; Oyedun et al., 2013; Choi et al., 2016), and biomass (Oyedun et al., 2012). The focus in these studies was on separating the wax-like PE products from the aqueous phase and oxygen-containing aromatics from cellulose decomposition (Korkmaz et al., 2009), reducing the energy demand for the endothermic pyrolysis process (Korkmaz et al., 2009; Cheung et al., 2011; Oyedun et al., 2012), and the selective separation of sulfur from the generated pyrolysis oil (Choi et al., 2016). Other authors conducted further research with plastics, specifically investigating the dechlorination of plastic mixtures consisting of PE and PVC (Fukushima et al., 2010) and PE, PP, PS, PET, and PVC (López et al., 2011; Lopez-Urionabarrenechea et al., 2012). Lopez et al. emphasized the importance of reflecting the complex waste composition with the applied polymer mixture. Nevertheless, Lopez et al. excluded nitrogen-containing polymers from their study. With their more complex, oxygen-containing feedstock mixture, the application of a thermal (López et al., 2011) and catalytic (Lopez-Urionabarrenechea et al., 2012) second pyrolysis stage was compared. Other studies provided further insights into the fundamentals of the dechlorination step of PVC (Yuan et al., 2014; Yin et al., 2021) or confirmed the effectiveness of chlorine removal by temperature staging in bench-scale experiments with polyolefin-rich waste (Park et al., 2018; Park et al., 2019; Park et al., 2022).

Recent studies have investigated staged pyrolysis of mixed plastic waste, focusing on deoxygenation, dechlorination, and selective product enrichment. Sophonrat et al. applied the staged pyrolysis concept to a

mixture of PE and PS contaminated with paper, PET, and PVC. In doing so, they were able to demonstrate deoxygenation of the wax-like product fraction and the separation of water from this target product (Sophonrat et al., 2018). Chang et al. investigated the concept of temperature staging with a mixture that also contains ABS in addition to PE, PP, PS, and PVC (Chang et al., 2023). As in previous studies, the focus lay on the dechlorination of the feedstock in a first stage. The enrichment of aromatic compounds for styrene monomer recovery and the production of an aliphatic-rich product fraction was pointed out. The fate of nitrogen-containing compounds played only a minor role in this study.

Interactions in polymer mixtures occurring during the reaction are considered to cause the shift in product composition. Possible interactions strongly depend on the polymer types and reaction conditions employed (Netsch et al., 2025, 2026; Williams and Williams, 1999). Thus, the type and content of different polymers in the feedstock are crucial for temperature-staged pyrolysis applications.

Reported investigations on uncatalyzed staged pyrolysis of thermoplastic mixtures are limited in the literature. These studies often refer to binary or ternary model mixtures and mostly aim at dehalogenation. Only a few of these studies examined real waste streams (Bockhorn et al., 1999; Park et al., 2022) or more complex feedstock mixtures that incorporate oxygen (López et al., 2011; Lopez-Urionabarrenechea et al., 2012; Sophonrat et al., 2018). One study covers nitrogen-containing polymers (Chang et al., 2023) but lacks information on denitrogenation effectiveness by temperature-staged processing. Thus, it remains unclear whether temperature-staging represents an appropriate method for optimizing polyolefin-rich mixed plastics from a circular economy perspective. This optimization aims to enrich heteroatoms and aromatics in one oil fraction while producing a high-quality aliphatic product suitable for reintegration in the (petro-)chemical industry for cracker applications.

Therefore, this study extends the concept of temperature staging to a broader feedstock spectrum. The aim is to produce aliphatic-rich pyrolysis oils of low oxygen-, nitrogen-, and chlorine-containing HCs and aromatics content. These contaminations should be transferred to a product fraction produced in the first pyrolysis stage, generated at a lower temperature. Additionally, the concept of temperature staging is tested in two different process scales to investigate the temperature control and scale-up challenges. Therefore, pyrolysis experiments are performed in laboratory-scale TG experiments and under technical conditions in a STR. The TG experiments offer the advantage of well-controlled conditions for a reliable parameter study. They enable the evaluation of the pyrolysis behavior in defined thermoplastic mixtures, considering possible interactions and reaction mechanisms. The potential of a temperature staging approach for optimizing the products of mixed plastic pyrolysis is then assessed in the STR system, based on the product yield and the composition of the resulting gas and pyrolysis oil. Temperature control and heat transfer effects are revealed, addressing crucial engineering aspects in stepwise pyrolysis. Mixtures of the eight most common thermoplastics are tested (PlasticsEurope, 2024). With PET, PVC, ABS, and PA6, the most critical contaminations, oxygen, chlorine, and nitrogen are included to reflect the diversity of plastic waste compositions and the associated impurities in the pyrolysis products (Kusenberg et al., 2022).

2. Materials and methods

2.1. Feedstock

Various thermoplastics were used as pure plastics and in defined thermoplastic mixtures. These included low-density polyethylene (LDPE, Lupolen 2420H by LyondellBasell), high-density polyethylene (HDPE, Hostalen ACP 9255 Plus by LyondellBasell), PP (Moplen HP 552H by LyondellBasell), PS (Ineos Styrolution 156F), PET (PKKPET by Plastipak Preforme), PA6 (Alphalon 27 by Grupa Azoty ATT Polymers), ABS (Sinkral F332 by Eni Versalis), and PVC. These materials were already used for kinetic analysis via dynamic TG (Netsch et al., 2025). Except for PVC, the polymers were supplied as additive-free primary granulates with a particle size of 2–5 mm. Mexichem provided the PVC (Primex P-2252) as a powder. It is referred to as virgin PVC in this study. In addition to pure polymers, various mixtures of thermoplastics were applied in TG. For technical reasons, a different PVC was used in STR experiments. For technical reasons, a different PVC was used in STR experiments. The powder caused clogging during the feeding process in the STR experiments because of its small particle size. Therefore, it was necessary to switch to PVC granulate in these investigations. This PVC by INEOS Inovyn was available as granulate with a particle size of 3 mm, but contained about 10 wt.% inorganic fillers such as $CaCO_3$ and TiO_2, as well as 2–3 wt.%. The stabilizers are not specified in detail by the manufacturer. In the following, this PVC is referred to as PVC granulate. In these STR experiments, the PVC granulate is examined in combination with other thermoplastics as a mixture, which is referred to as STR Mix in this study. This mixture contains 50 wt.% LDPE, 15 wt.% PP, 10 wt.% each of PS and PET, and 5 wt.% each of PA6, ABS and PVC granulate. It has already been used in isothermal STR experiments. The feedstock composition, including elemental composition, ash, and moisture content, was determined in a previous study and is summarized in Table 1.

2.2. Thermogravimetry

TG analyses were performed with a NETZSCH TG 209 F1 Libra. An automatic sampler was used to load the microbalance with Al_2O_3 crucibles containing 10 mg of sample. Before loading, the samples were cut from the primary granulate with a scalpel. The total sample mass only deviated by up to 0.1 mg. In addition to the pure plastics, binary and ternary thermoplastic mixtures were investigated. In binary mixtures, equal amounts of the polymer types were employed. The ternary mixtures comprised 30 wt.% of the first and second polymer types, as well as 40 wt.% of the third polymer under investigation. Additionally, a complex mixture containing 20 wt.% each of LDPE and HDPE, as well as 10 wt.% each of PP, PS, ABS, PET, PA6, and PVC, was tested and labeled as TG Mix in the following. The polymer content deviation in the mixtures ranged from 10 to 15 µg at maximum. The experiments were conducted at least twice for each mixture. The oven temperature was programmed from 30 °C to 900 °C with simultaneous purging at 60 ml/min nitrogen. Within this program, isothermal segments were applied, pausing the dynamic heating rate of 10 K/min. The selection of the heating rate, the segment's hold time, and its isothermal temperature was based on the results of a previous study under dynamic TG conditions (Netsch et al., 2025). The heating rate of 10 K/min ensured well-controlled conditions without the influence of temperature gradients. Also, the reported polymer-specific decomposition onset temperatures, along with the associated decomposition kinetics, were considered (Netsch et al., 2025). The hold time varied between 0.5 h and 1 h for the

Table 1
Elemental composition as well as the moisture and ash content of the investigated feedstocks.

Feedstock	Composition in wt.%						
	C	H	N	Cl	Moisture	Ash	O [A]
LDPE	85.8	14.2	< 0.3	0.0	< 0.01	< 0.01	0.0
HDPE	85.8	14.2	< 0.3	0.0	< 0.01	< 0.01	0.0
PP	85.8	14.2	< 0.3	0.0	< 0.01	< 0.01	0.0
PS	92.0	8.0	< 0.3	0.0	< 0.01	< 0.01	0.0
ABS	86.2	8.0	5.5	0.0	0.3	< 0.01	0.0
PET	63.3	4.4	< 0.3	0.0	0.2	< 0.01	32.1
PA6	63.6	9.8	12.6	0.0	1.2	< 0.01	12.7
Virgin PVC	39.6	5.6	< 0.3	54.7	0.1	< 0.01	0.0
PVC granulate	36.2	4.9	< 0.3	47.9	0.2	10.6	0.2
STR Mix [B]	80.6	11.6	0.9	2.4	0.1	0.5	3.9

[A] organic oxygen calculated as the difference to 100 wt.%.
[B] calculated from the individual polymer content in the mixture.

selected isothermal temperatures of 300 °C and 370 °C, respectively. The lower temperature segments enabled the investigation of the dechlorination process induced by the first step of the two-step PVC pyrolysis reaction mechanism. The defined decomposition of PS, ABS, PET, and PA6 was assessed by implementing the segment at 370 °C. The pyrolysis of polyolefins and the polyene chains, formed during the PVC dichlorination, followed in the third pyrolysis stage. The temperature increase after the 370 °C segment marked the beginning of this third stage. The systematic TG study also involved other isothermal segment temperatures and deviating hold times. Supplementary information S1 provides an overview of all experimental setups that were tested but not shown in the manuscript, including the applied polymer mixtures and temperature programs.

2.3. Stirred tank reactor

Complementing the experiments under well-controlled conditions in the TG, the STR system offered additional investigations, as technical process conditions prevail here. This includes reactor-design effects known from large-scale pyrolysis plants, such as relevant heat and mass transport limitations or product residence time distributions. The system is also characterized by high feedstock and process flexibility. It has been described in detail by Netsch et al. for experiments with various thermoplastics and post-consumer waste at a constant reactor temperature of 500 °C (Netsch et al., 2026). The reactor had a capacity of 2.7 L and was electrically heated by two heating sleeves with each 1.25 kW power. A customized impeller enabled fast homogenization of the reactor content. Quartz sand was used as a homogenization agent. Nitrogen was supplied at various points of the reactor system to ensure an inert atmosphere, transfer emerging volatile products to the condensation system, and avoid blockages on critical system parts. The condensation system consisted of two parts, each including two double-tube heat exchangers. The first and second parts were maintained at 60 °C and –5 °C, respectively. An electrostatic precipitator prevented the transfer of droplets in the potentially oversaturated aerosols from the last condensation stage to the downstream gas sampling and analysis section of the pyrolysis system. This section enabled gas sampling for offline analysis and online analysis of the gas volume flow throughout the experiment. As toxic, corrosive, carcinogenic, and environmentally harmful substances were expected to form during pyrolysis, the experiments were conducted following high health and safety measures. The mass balancing was performed using the methodology already applied and validated in isothermal tests on this pyrolysis system (Netsch et al., 2026). A feedstock mass of 0.25 kg was introduced to the reactor in batch operation. Two-staged pyrolysis at different temperatures of the first stage was investigated in the STR system. The reactor, containing 2 kg of quartz sand, was preheated to the first isothermal temperature and held for at least one hour after the introduction of the feedstock. This isothermal temperature was varied at 370 °C, 400 °C, and 430 °C to evaluate the influence of increasing this temperature, starting from the set parameter investigated in TG. Following this stage, the reactor set temperature was increased to the second pyrolysis stage temperature of 500 °C and maintained for an additional 90 min to ensure complete conversion. Thermocouples on the reactor wall and in the interior of the reaction mixture allowed recording of the temperature profile and thus resolving the temperature gradients occurring between the reactor wall and the reaction zone. The STR system is characterized by intense mixing in the reaction zone and a narrow gas residence time distribution with a minimum gas residence time of less than 20 s (Netsch et al., 2026). For comparison, unstaged isothermal pyrolysis experiments at a set temperature of 500 °C were conducted using the same reactor system. However, the experiments differed in the feedstock dosing procedure. The feedstock was introduced semi-continuously in small quantities of about 30 g into the preheated reactor at 500 °C to ensure stable temperature conditions.

2.4. Analytics

To evaluate the valuable organic products, they were characterized using comprehensive offline analysis methods. An advanced gas chromatography (GC) system was used for the pyrolysis gas characterization. This system comprises an Agilent 8890 GC combined with an isothermal oven, a thermal conductivity detector (TCD), a flame ionization detector (FID), and a mass spectrometer (MS).

Gas samples were taken at various times during the experiment and analyzed. The system enabled the quantification of N_2, O_2, CO_2, CO, and CH_4 using the TCD. Other HCs were identified with the MS and quantified using the FID signal after calibration. HCl causes no distinct peak in the measuring system, but only a broad increase in the baseline as a result of its strong tailing tendency. The peak can be clearly attributed to HCl using the MS. However, reliable peak integration is not possible, thus preventing quantitative evaluation of HCl. A mass-related composition of the permanent gases is calculated from the other quantified gases. The calculation is performed in the first step by determining the volume-related proportion of the respective component y_i, considering the molar volume V_m under standard conditions (0 °C, 1 atm), the quantified concentration c_i, and the molar mass M_i of the respective gas, following equation (1).

$$y_i = c_i \frac{V_m}{M_i} \tag{1}$$

The sum of the volume fractions is normalized to correct for measurement deviations. The mass fraction of a gas species related to the permanent gas $x_{i,permanent\ gas}$ is then calculated using the density of the permanent gas $\rho_{permanent\ gas}$ and the gas species ρ_i, as shown in equation (2).

$$x_{i,permanentgas} = \frac{y_i}{\sum_i y_i} \bullet \frac{\rho_i}{\rho_{permanent\ gas}} \tag{2}$$

Finally, the purge gas in the form of nitrogen is excluded from the composition by subtracting its mass fraction $x_{flush\ gas}$ from the sum of mass fractions of all quantified gas species. The mass fraction related to the pyrolysis gas $x_{i,Pygas}$ is calculated as described in equation (3). Further details on the GC system and the calibration methodology are provided elsewhere (Chang et al., 2023).

$$x_{i,pygas} = \frac{x_{i,permanent\ gas}}{\sum_i \left(x_{i,permanent\ gas}\right) - x_{flush\ gas}} \tag{3}$$

Elemental analysis, determination of water content, spectroscopy, and GC analysis are performed for pyrolysis condensate characterization. A micro elemental analyzer type LECO Truspec CHN was used for elemental analysis. The measurement uncertainty of the elemental analysis differs regarding the sample type and the determined element. For the polymers, a maximum uncertainty of less than 0.46 wt.% for carbon, 0.13 wt.% for hydrogen (0.47 wt.% in case of PVC), 0.05 wt.% for nitrogen, 0.01 wt.% for moisture, and 0.04 wt.% for ash determination were ascertained. For chlorine, the uncertainty accounted for 0.41 wt.% and 0.16 wt.% in the case of virgin PVC and PVC granulate, respectively. Elemental analyses of pyrolysis oils exhibit maximum uncertainties of 1.00 wt.% for carbon, 1.02 wt.% for hydrogen, 0.07 wt.% for nitrogen and chlorine, and 0.11 wt.% for moisture.

Karl Fischer titration was conducted with a Methohm 870 KF Titrino following DIN 51777. ^{1}H NMR analyses were carried out using an 80 MHz Magritek Spinsolve MultiX benchtop nuclear magnetic resonance (NMR) spectrometer. The NMR analyses indicate the distribution of differently bound ^{1}H-nuclei, also referred to as protons. This allows the examination of condensates from different stages regarding their share of aromatic bonds as well as saturated and unsaturated C-C bonds. The condensates were measured with a two-dimensional GC (GCxGC) method. All setups and methods are already described in detail by Netsch et al. (Netsch et al., 2025).

3. Results and discussion

3.1. Thermogravimetric analyses

3.1.1. Virgin polymers

The decomposition behavior of the polymers is characterized under well-controlled TG conditions. The time- and temperature-dependent sample mass change is recorded to resolve the progression of the pyrolysis reaction by the formation of gaseous and condensable products. TG experiments with virgin polymers exhibit the conversion rate of individual polymers in the selected isothermal segments. These segments are set to 300 °C and 370 °C. The temperatures were maintained for 30 min and 60 min, respectively. The results are shown in Fig. 2.

A significant mass loss during the 300 °C stage is only evident for PVC. The decomposition of PVC starts even before reaching the isothermal temperature. At the end of the segment, about 61.4 ± 0.1 wt. % of volatiles are released. The results emphasize the dichlorination reactions occurring in PVC at low temperatures below 300 °C (Yu et al., 2016). In the second stage, the reactions of PVC pyrolysis slow down, leading to a minor volatile release of only 7.3 ± 0.1 wt.%. As the temperature rises, the polyene chains pyrolyze at temperatures above 400 °C. This results in the additional release of volatile products and coke formation. The coke amounts to 6.2 ± 0.1 w.t%. In the second stage, at 370 °C, the non-polyolefinic thermoplastics degrade according to the kinetics that were characterized in the dynamic experiments shown in Fig. 1. While HDPE only degrades to approximately 3 wt.% until the end of the second isothermal segment, the decomposition of PS, ABS, PET, and PA6 is pronounced. The PS decomposition results in nearly complete conversion at the end of the stage. Here, the formation of volatiles from ABS, PET, PA6, and PP pyrolysis reaches 77.3 ± 0.1 wt. %, 51.1 ± 0.3 wt.%, 43.6 ± 1.8 wt.%, and 16.8 ± 0.1 wt.%, respectively. This partial decomposition reflects their slower pyrolysis kinetics at 370 °C compared to PS. Only for PET and PVC, significant coke formation can be detected at the end of the experiment. The coke amounts to 12.9 ± 0.2 wt.% in the case of PET. PP features a partial decomposition in this stage.

These TG results show remarkably different reaction rates, depending on the polymer type in the sample. Applying a higher temperature or extending the hold time raises the conversion rate of all thermoplastics. A distinct temperature cutoff for separating the pyrolysis of aromatic or heteroatom-containing polymers from the pyrolysis of polyolefins cannot be identified. The overlapping of decomposition ranges, especially for PP and PS, leads to a transitional effect. Instead of a clear separation, this suggests an enrichment or depletion of specific decomposition products by temperature-staging. Nevertheless, a temperature range between 370 °C and 400 °C may offer the possibility of partially separating the polyolefin decomposition from the decomposition of other polymers. In the following, this temperature range between 370 °C and 400 °C is referred to as the kinetic gap and will be focused on.

3.1.2. Polymer mixtures

Some authors report polymer interaction effects that occur during pyrolysis (Netsch et al., 2025; Williams and Williams, 1999; Cao et al., 2023; Jing et al., 2013). These effects depend on the polymers that interact in the feedstock and can vary in intensity. In particular, the impact of interactions on the reaction rate is relevant for the application of temperature-staged pyrolysis. Possible deceleration or acceleration during the co-pyrolysis of polymers could limit or extend the kinetic gap between polyolefins and other thermoplastics. To evaluate such effects, the complexity of the feedstock mixture is increased through experiments performed with binary and ternary mixtures, and the TG Mix. Fig. 3 shows the TG result of a ternary mixture of polyolefins in a three-staged pyrolysis with isothermal segments at 300 °C and 370 °C. A mixture of PP, LDPE, and HDPE was tested in a proportion of 30 wt.%, 30 wt.%, and 40 wt.%, respectively. No volatile formation and only minor decomposition occur in the ternary polyolefin blend at both temperature stages. Approximately 10.9 ± 0.1 wt.% of volatiles are released from the sample by the end of the 370 °C stage. A comparison of the calculated and the experimental TG curves of this mixture can be found in the supplementary information in Fig. S1.1. These results rely on the determination according to the proportions of the polymers in the mixture. Based on the pure polymer results, only 7.8 ± 0.1 wt.% of released volatiles is calculated. Compared to the experimental results, this value is about 3.0 wt.% lower, indicating a slight acceleration. The slight acceleration may be attributed to interactions as reported by Jing et al. (Jing et al., 2013). Radicals formed during the PP pyrolysis may also serve as initiation radicals in the radical decomposition mechanism of PE (Bockhorn et al., 1999). Nevertheless, the absolute impact is low as the majority of the pyrolysis products are formed at higher temperatures. No or only minor deviations comparable to those of the polyolefinic ternary mixture are observed for other mixtures of polyolefins with PET, PA6, or ABS. This isothermal TG result confirms the absence of significant interactions in these samples, as reported in a previous TG study under dynamic parameter conditions (Netsch et al., 2025).

Exemplary results of PS blended with PET, PA6, PP, and HDPE are depicted in Fig. 3, too. For mixtures of PS and polyolefins, no considerable interactions were found based on the theoretical calculations of pure polymer decomposition, which confirms findings of blends comprised of PS and both PE types from other authors (Faravelli et al., 2003; Westerhout et al., 1997). The mixtures of PS/PET/HDPE and PS/

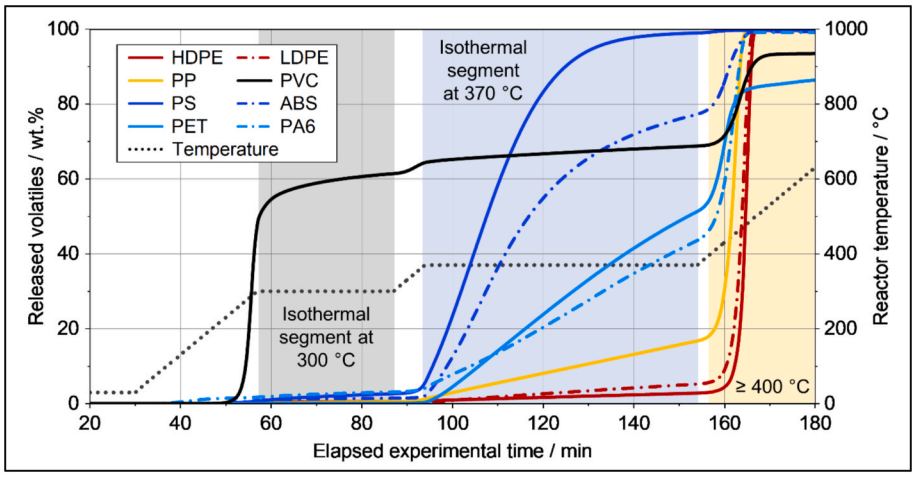

Fig. 2. Individual three-staged TG experiments conducted for virgin polymers at isothermal segments for PVC dichlorination at 300 °C (grey), decomposition of aromatic-based and heteroatom-containing polymers at 370 °C (blue), and polyolefin decomposition above 400 °C (yellow).

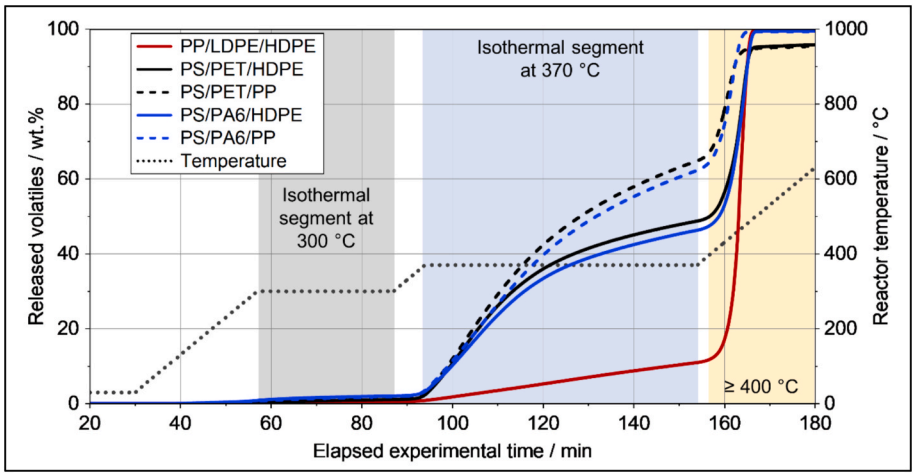

Fig. 3. Three-staged TG experiments with isothermal segments at 300 °C for 0.5 h (blue) and 370 °C for 1 h (blue) performed with ternary mixtures in the proportion of 30/30/40 wt.%.

PA6/HDPE release 47.9 ± 1.2 wt.% and 46.5 ± 0.3 wt.% of volatiles by the end of the second stage. From pure polymer decomposition, a volatile formation of 46.1 ± 0.2 wt.% and 43.9 ± 0.6 wt.% would be expected. The calculated and the experimental TG curves are depicted in Fig. S1.2 in the supplementary information. The similar values emphasize that interactions only play a minor role in these blends. In contrast, the reaction of a mixture containing PS and PP is accelerated compared to the values calculated from the individual polymer behavior. For PS/PET/PP and PS/PA6/PP, about 62.9 ± 2.7 and 62.3 ± 2.5 wt.% of volatiles are formed after the 370 °C stage, compared to the calculated volatile formation of 51.7 ± 0.2 and 49.4 ± 0.6 wt.%, respectively. The calculated decomposition results are compared to the experimental values in Fig. S1.3 in the supplementary information.

The radicals formed in the initiation step of the pyrolysis of PP and PS provide starting radicals for the other polymer. This effect is very pronounced in PS/PP blends, as already described by Kruse et al. (Kruse et al., 2005). It is also observed in the co-pyrolysis of PE and PS (Costa et al., 2010). The data under comparative experimental conditions for both mixtures of this study suggest, though, that the accelerating effect is less pronounced in PS/PE blends than in PS/PP blends. The similar pyrolysis set temperatures of PS and PP, which are based on more stable radicals in the initiation phase of decomposition, might explain this. The positive inductive effects of the phenyl or methyl substituents in PS and PP are a potential cause for this effect. Additionally, Faravelli et al. point out that this effect in polyolefins and PS strongly depends on the mixture of polymers in the reactor system (Faravelli et al., 2003). Yet it can be assumed that the polyolefin chains decompose more intensely in the first stage. This effect of accelerated polyolefin decomposition in the presence of PS is disadvantageous, as it narrows the kinetic gap between PS and polyolefins. This would complicate the enrichment of aliphatic target products or the depletion of contaminants upon implementation of the temperature-staged pyrolysis concept.

The most intensive interactions are found in mixtures of PET, PA6, and PVC. To illustrate this, the decomposition of the TG Mix and exemplary ternary mixtures are shown in Fig. 4. Ternary mixtures with 30/30/40 wt.% proportions of PVC/PET/PP, PVC/PA6/PP, and PET/PA6/PP reveal different effects important for temperature staging. If a mixture contains at least two of the polymers PVC, PET, and PA6, a distinct acceleration of the decomposition occurs, as already described by dynamic TG tests with binary mixtures (Netsch et al., 2025). This acceleration enhances the volatile formation during the first stage of dechlorination. It is more pronounced for blends of PVC with PA6 than with PET. The underlying mechanisms for the co-pyrolysis of PVC with PET are mechanistically explained by Cao et al (Cao et al., 2023). According to the authors, the formation of hydrogen chloride at the initial PVC decomposition stage promotes the C-O bond cleavage in the polyester group of the PET polymer backbone. A detailed mechanistic description of the interactions between PVC and PA6 blends has yet to

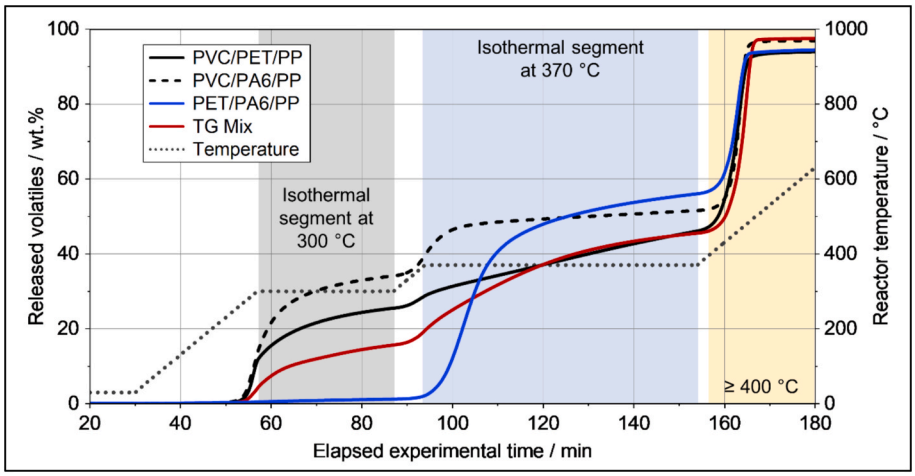

Fig. 4. Staged TG experiments with isothermal segments at 300 °C for 0.5 h (grey) and 370 °C for 1 h (blue) performed with ternary thermoplastic mixtures in the proportion of 30/30/40 wt.% and the TG Mix.

be provided. In the PET and PA6 mixture with PP, no volatile formation is evident in the first stage of 300 °C, but about 55.8 ± 0.3 wt.% of the blend pyrolyzes into volatile HCs in the second stage. From pure polymer decomposition, only 35.1 ± 0.7 wt.% of released products are expected. This finding emphasizes that PET and PA6 can interact during pyrolysis, causing faster decomposition. The entire calculated TG curve is shown in Fig. S1.4 in the supplementary information.

Furthermore, the pyrolysis at temperatures above 400 °C exhibits a minor shift of the degradation curve towards higher temperatures when using PVC and polyolefin blends. The high-temperature decomposition of polyene chains formed as intermediates during PVC decomposition slightly delays the polyolefin pyrolysis during the co-pyrolysis (Yu et al., 2016). Together, both effects broaden the kinetic gap, facilitating the separation of the non-aliphatic and aliphatic pyrolysis products by temperature staging. Nevertheless, the interaction of PVC and polyolefins also leads to slightly lower aliphatic product yields because of the intensified coke formation (Yu et al., 2016).

In the complex TG Mix, the described interaction effects overlap simultaneously. During the dechlorination phase of PVC at 300 °C, twice the proportion of volatiles is released in comparison to the expected behavior from pure polymer decomposition. By the end of this stage, 15.7 ± 0.0 wt.% of volatiles are formed. Only 7.0 ± 0.0 wt.% was expected, emphasizing the decomposition interactions of PVC with PET and PA6. The calculated decomposition curve of the TG Mix is depicted in Fig. S1.5 in the supplementary information in detail. The proportion of pyrolysis products formed within the second stage is also increased by approximately 8 wt.% and amounts to 45.0 ± 0.8 wt.%. This corresponds to the polyolefin content of 50 wt.%. Based on the TG results, nearly complete decomposition can be assumed under the conditions applied. In conclusion, the TG results provide precise information on the interaction effects that can be attributed to specific polymer combinations. They explain how the decomposition kinetics of mixed thermoplastics are affected, whether they are accelerated or slowed down, and what impact this has on temperature-staged pyrolysis. In the TG Mix, some interactions are favorable due to the accelerated decomposition of the heteroatom-containing polymers as seen in PA6, PET, and PVC mixtures. The decomposition of the polyolefins differs depending on the mixture. PS accelerates, and PVC slightly inhibits their pyrolysis.

The yield and quality of the targeted product, the aliphatic-rich oil fraction, from the final pyrolysis stage are crucial for optimization of process parameters. Hypothetically, low temperature and hold time of the second decomposition stage (here at 370 °C) are beneficial for maximum pyrolysis condensate yield in the second stage, as minor amounts of polyolefins already decompose in the second stage. As the yield of the aliphatic-rich fraction increases, a higher conversion efficiency into the targeted product is achieved. Simultaneously, more pyrolysis products from the decomposition of PS, ABS, PET, and PA6 end up in this product, presumably reducing its quality. Consequently, the selectivity to aliphatic compounds in the products of the last stage is lower. With this, TG results imply that a simultaneous improvement in conversion efficiency and conversion selectivity is not possible. The selection of optimal parameters for temperature-staged pyrolysis thus depends on whether the objective is to maximize the target product yield or to achieve a high target product quality. Nevertheless, temperature-staged pyrolysis in complex mixtures can be assessed as a technically feasible option for improving the pyrolysis product under TG conditions from a kinetic point of view. However, temperature staging can only enable selective product enrichment or depletion rather than perfect separation. Based on these results, the scale-up of the concept was investigated employing a STR system, since additional tests under realistic pyrolysis conditions, along with further comprehensive product analyses, are required.

3.2. Stirred tank reactor

The well-defined set parameters from TG experiments might need adjustment in application to technical reactors to achieve a similar product separation effect. The application was examined in the scalable STR system. These experiments enabled mass balancing and in-depth chemical product analyses. Since an aliphatic-rich pyrolysis oil is the targeted product, only a two-staged pyrolysis is performed in contrast to the TG experiments. The first stage should ensure complete dichlorination and the removal of heteroatoms and aromatic compounds in one step. From the second stage, the aliphatic-rich product fractions are obtained. Based on previous studies with the STR system, a constant pyrolysis temperature in the reaction zone cannot be assumed for batch operation with 250 g feedstock, due to heat and mass transfer limitations (Netsch et al., 2026). However, the temporal progression of the effective temperature in the STR mix is decisive for its kinetics and, therefore, the result of the temperature staging. Fig. 5 displays the time–temperature dependence of the reactor wall and the reaction zone during the experiments. After feedstock dosing, a significant temperature decline of about 140 °C was recorded in the reaction zone in both experiments. The reactor wall temperature remained stable, only varying approximately 5 °C. During the hold time of the isothermal segment, the reaction temperature increased to its set temperature in 20 min. The isothermal segment in the experiment was maintained at a higher temperature of 430 °C for 90 min. To compensate for the previously discussed drop at the 400 °C stage, the increase in reactor temperature started after 96 min. In both experiments, the internal reactor temperature followed the reactor wall temperature slowly until a stable internal temperature was reached. This temperature was approximately 10 to 25 K below the specified reactor wall temperature of 500 °C.

In the reference experiment, the feedstock was introduced semi-continuously in small portions (approximately 30 g) to maintain a stable pyrolysis temperature, whereas a single-step addition was used in the staged experiments to precisely control reaction time and temperature. The total feedstock mass is identical in both cases. The difference in dosing strategy exhibits only minor effects on the polymer temperature profile. The time-dependent polymer temperature profile mainly depends on the temperature program, rather than on the initial temperature decline upon feedstock addition. Therefore, the staged and reference experiments are comparable for assessing product distribution and reaction kinetics.

The results demonstrate how temperature gradients in the technical system and endothermic processes such as feedstock heating, phase transitions, or reaction enthalpy influence the time-dependent polymer temperature during plastics pyrolysis. This temperature is decisive for

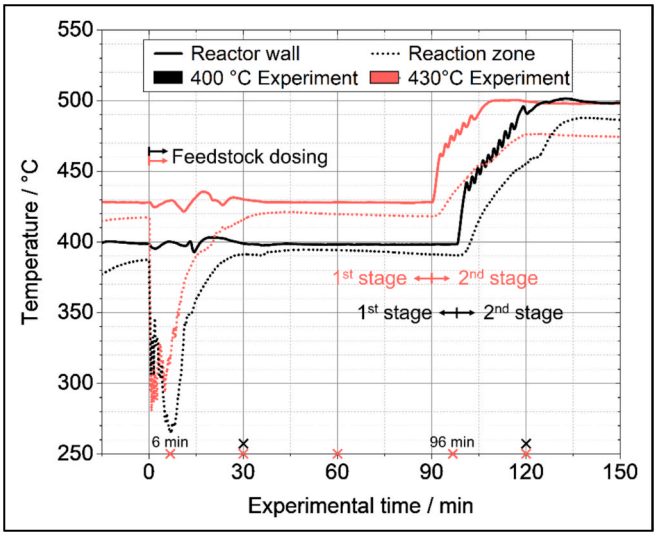

Fig. 5. STR reaction zone and reactor wall temperature during the temperature-staged pyrolysis of the STR Mix with isothermal segments at 400 °C and 430 °C, including gas sampling marked with a cross on the x-axis.

the reaction kinetics. Higher stage set temperature and longer hold time of the isothermal segments must thus be applied in the STR system to achieve comparable reaction conditions in both systems.

3.2.1. Mass balance

The mass balance provides information on the yields of the product fractions, which are referred to as pyrolysis gas, pyrolysis oil, and solid residue in the following. Generating a high oil yield is required to optimize the recycling process for pyrolysis condensate utilization. At the same time, this condensate phase ideally contains no heteroatoms and is rich in saturated aliphatic compounds. For this purpose, oxygen-, nitrogen–, chlorine-, and aromatic-containing products should be predominantly transferred to the gas phase or enriched in the separately collected condensate of the first stage of the pyrolysis process. On the one hand, both effects lead to a depletion in the target product. On the other hand, it would inevitably reduce the condensate yield. As already concluded from TG results, the general optimization task aims to simultaneously improve the product composition while maintaining the highest possible condensate yield. Table 2 shows the condensate yields obtained in the STR Mix two-stage pyrolysis experiments compared to an experiment at a constant temperature of 500 °C (Netsch et al., 2026). For technical reasons, only the condensate yield can be distinguished by the respective stages. Pyrolysis gas and solid residue are calculated for the entire experiment. Furthermore, an experiment not listed in Table 2 with an isothermal segment at 370 °C for 90 min was performed. This experiment showed no relevant condensate formation during the first stage. Only slight PVC dehalogenation was observed in this 370 °C test run, and low amounts of gases were detected. Insufficient condensate mass for further condensate analysis was obtained during the primary pyrolysis stage of the 370 °C experiment. Therefore, this experiment was neglected for evaluating the mass balance and product compositions.

All pyrolysis experiments of the STR Mix exhibit a similar mass balance. The gas yield of the staged pyrolysis results is slightly lower with 4 wt.% compared to the reference experiment at 500 °C under semi-continuous feedstock dosing. Accordingly, the yield of the solid fraction and the collected pyrolysis oil increase by approximately 1.5 wt.% and 2–2.5 wt.%, respectively. The polymers that predominantly decompose at lower temperatures, such as PS, ABS, PET, PA6, or PVC, are pyrolyzed in the first stage. This temperature was about 70–100 °C lower compared to the unstaged reference experiment at 500 °C. With a lower pyrolysis temperature, reduced formation of pyrolysis gas is reported (Calero et al., 2023; Chang, 2023). Thus, a shift in product distribution towards high-molecular products, and consequently from the gas phase to the condensate phase, is expected for the staged pyrolysis experiments. The mass balance results agree with the reported finding (Calero et al., 2023; Chang, 2023). Conversely, pronounced solid residue formation is commonly reported for increasing pyrolysis temperatures (Maqsood et al., 2021). However, an elevated solids residue yield during co-pyrolysis of mixed plastics results from interactions between coke-forming polymers and non-coke-forming polymers (Netsch et al., 2025; Williams and Williams, 1999). Such interactions may cause coke formation by incorporating products of non-coke-generating polymers into polyaromatic coke precursors. Slower reaction kinetics as a consequence of the lower pyrolysis temperature lead to more time for interactions in the melt phase of the molten polymer mixture, which may explain the slight increase observed in this study.

The comparison of the pyrolysis oil yield of the different stages reveals significant differences, as indicated in Table 2. Increasing the hold temperature from 400 °C to 430 °C results in an increase in the condensate yield in the first stage by about 20 wt.%. The temperature increase accelerates the decomposition reactions, resulting in a higher feedstock conversion. The higher condensate yield during the 430 °C stage reduces the yield of the target product, but might improve the pyrolysis oil quality by enhanced conversion of PS and the heteroatom-containing polymers. Based on the condensate yield of 2.9 wt.% in the first stage of the 400 °C test, only partial pyrolysis can be expected for these polymer types in the thermoplastic mixture.

Table 2
Mass balance of the staged pyrolysis experiments of the STR Mix with an end temperature of 500 °C compared to the pyrolysis at 500 °C in the STR.

Experiment	Product fraction yields in wt.%		
	Gas	Oil	Solid Residue
Isothermal 500 °C (Netsch et al., 2026)	41.3	55.1	3.6
Two-stage pyrolysis (400 °C for 96 min, 500 °C for 90 min)	37.8	57.0 1st stage: 2.9 2nd stage: 54.1	5.2
Two-stage pyrolysis (430 °C for 90 min, 500 °C for 90 min)	37.2	57.6 1st stage: 22.3 2nd stage: 35.3	5.2

3.2.2. Gas product composition

The gas analyses support assessing the efficiency of the staged pyrolysis setup in the STR. The gas composition is measured at defined times during both staged pyrolysis experiments, as shown in Fig. 4. In the test with a 400 °C stage, samples are taken after 30 and 120 min, while in the test at 430 °C, samples are collected after 6, 30, 60, 96, and 120 min. The samples provide information about compositional changes in the gas during the reaction progress. Fig. 6 presents different gaseous product groups in the staged test at 430 °C as a function of the sampling time. These products are characteristic pyrolysis products of the individual thermoplastic polymer types in the mixture. The chromatograms and their corresponding quantitative gas compositions can be found in Supplementary Information S2. The gas composition of the temperature staging experiments at 400 °C confirms the observations seen in the more frequently sampled test at 430 °C holding temperature.

Aliphatic products, aromatics, CO_2, and CO dominate the integral gas composition. However, the gas analysis reveals distinct shifts in the gas composition depending on the sampling time. The CO_2 and CO contents decrease rapidly during the experiment and reach a stable level of 2 wt.% by the end of the isothermal segment of the staged pyrolysis. At the same time, the aliphatic content increases during the experiment and amounts to approximately 90 wt.% after 60 min. Only a few aliphatics are present in high amounts in the gas sample collected after 6 min, with 29.8 wt.% ethene and 5.3 wt.% methane. In the sample obtained after 30 min, this distribution becomes significantly broader. Branched C_3-, C_4-, C_5- and C_6-HCs dominate. This trend continues up to the gas sample taken at 60 min. Once the temperature is increased to 500 °C, higher proportions of methane, ethene, and ethane are recorded in the pyrolysis gas, broadening the distribution. Among the aliphatic components, n-alkanes and α-olefins appear in addition to the branched HCs after 60 min. The content of aromatics increases from 4.6 wt.% (6 min) to 14.0 wt.% (96 min) during the test. This maximum is reached following the end of the isothermal segment at 430 °C. At 120 min, the aromatic content has already declined. At 6 min, more benzene and hardly any toluene are detected. The toluene content then increases steadily to the sample withdrawn at 96 min. About 7 wt.% of toluene is detected before decreasing again. The styrene content remains almost constant at 2.1 to 3.5 wt.% over the entire test. Minor amounts of chlorine-, nitrogen-, and oxygen-containing HCs are also identified in the pyrolysis gas. HCl, as the main gaseous decomposition product of PVC, is identified in the sample taken after 6 min. Because of the pronounced peak tailing, it cannot be accurately quantified using the GC system. Therefore, HCl is missing in the normalized composition. The oxygen- and nitrogen-containing HCs consist of acetaldehydes, acrylonitrile, and HCN. Low amounts of acetonitrile and methacrylonitrile are also detected. While high quantities of acetaldehyde are only present in the sample at 6 min, the proportion of nitrogen-containing HCs only decreases slowly with the progression of the isothermal segment. Thus, after an initial 1.0 wt.% of nitrogen-containing HCs, only 0.1 wt.% can

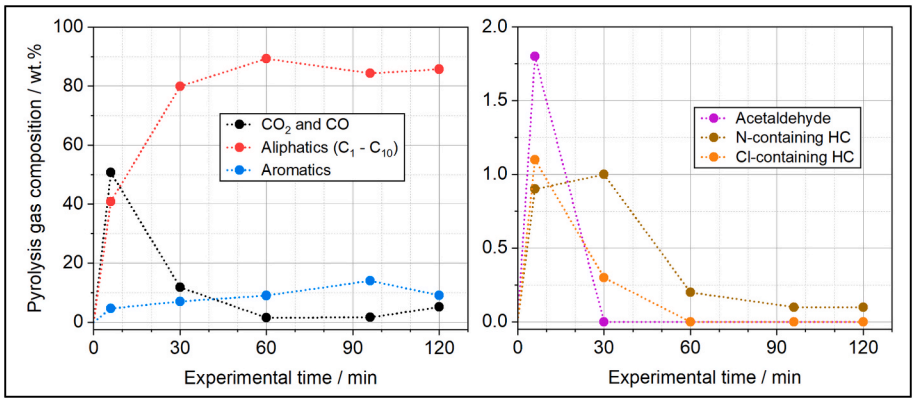

Fig. 6. Content of characteristic gas compounds sampled after 6, 30, 60, 96, and 120 min in the two-staged pyrolysis at 430 °C and 500 °C in the STR system.

be determined after the isothermal segment of the experiment. The chlorine-containing HCs are comprised of chloromethanes, chloroethanes, vinyl chlorides, 1,2-dichloroethanes, and chlorobutanes. These components are present in the 6 min gas sample predominantly. In the last gas sample of the isothermal segment (after 60 min), no more chlorine-containing HCs are detectable.

The gas analyses support the hypothesis that temperature-staged pyrolysis enables the separation of polymer-specific pyrolysis products. The typical gaseous PVC products are only recognizable at the start of the pyrolysis. With CO_2, CO, acetaldehyde, and ethylene, the results indicate an almost complete dichlorination of PVC and rapid decomposition of PET at the start of the experiment. Previously discussed interaction effects between PVC and PET may strongly accelerate the PET pyrolysis in the STR (Cao et al., 2023). Along with a high pentane content, the nitrile compounds indicate that PA6 and ABS also decompose at 430 °C during the isothermal segment. From 96 min on, more unbranched HCs are released beside the branched HCs. In the gas sample withdrawn after 60 min, the aliphatic C_4-C_{10} HCs consist of about 55 wt.% linear and 45 wt.% branched molecules. In samples taken at 96 min and 120 min, the proportion of branched C_4-C_{10} HCs declines to 40 wt.% and 27 wt.%, while the share of corresponding linear HCs rises to 60 wt.% and 73 wt.%, respectively. Thus, polyethylene appears to react in relevant quantities in the second stage, as assumed from the TG results. The TG results already identified the separation of PS and PP via temperature grading as the greatest engineering challenge. Relevant proportions of branched PP products are already apparent in the gas sample during the isothermal segment at 430 °C. This demonstrates that the decomposition of PS and PP is difficult to separate via temperature staging in the technical system. Their kinetics in the applied temperature range of 430 °C exhibit only slight reaction rate differences. The interactions between PS and polyolefins may further contribute to this effect. As a result, heteroatom-containing compounds can be efficiently enriched in the gas product during an isothermal pyrolysis stage. This applies to CO_2, CO, chlorine-, oxygen-, and nitrogen-containing HCs. The holding time of 90 min provides enough reaction time for their almost complete decomposition under the pyrolysis conditions. Nevertheless, an enrichment of aromatics in the first temperature stage can only be realized to a limited extent in the investigated pyrolysis system. Lowering the temperature delays all decomposition reactions, causing heteroatom-containing HCs formation for a longer experimental time. The gas analyses of the samples with a 400 °C step confirm this with higher quantities of heteroatom-containing HCs even after 30 min. In particular, nitrogen-containing HCs and aromatics from PS and ABS are present in the gas phase of the second stage in this test run. Although lowering the temperature would increase their yield in the second stage and above, more undesired HCs can be detected. Thus, the separation efficiency for gaseous species is reduced by lower temperatures.

3.2.3. *Condensable pyrolysis products*

The elemental composition reveals the mitigation of heteroatom-containing HCs into the condensable product fraction. Therefore, it allows for evaluating the potential enrichment of these oil species in the product obtained during the first isothermal pyrolysis stage. Table 3 lists the elemental analysis of the organic condensate obtained in the staged pyrolysis experiments.

The elemental analysis proves the enrichment of oxygen-, nitrogen-, and chlorine-containing HCs in the pyrolysis oil of the first pyrolysis stage. These chemical elements exceed the content of the pyrolysis oil in the isothermal reference test significantly. The water content in the condensate is also high in both condensate fractions. A comparison of the pyrolysis oil obtained in the first stage at the 400 °C and 430 °C experiments shows a higher carbon and hydrogen content than in the 430 °C condensate. This result supports the conclusion from the mass balance that relevant polyolefin decomposition occurs at the second pyrolysis stage. For the condensate fraction produced after the temperature increase, the heteroatom content is correspondingly lower.

Both pyrolysis oils that were obtained in the second stage at 500 °C exhibit a superior composition compared to the unstaged reference test at 500 °C. The comparison of both oils obtained from the staged experiments exhibits similar values with approximately 0.2-0.3 wt.% of nitrogen, chlorine, and oxygen. Some of the differences are already in the range of the measurement uncertainties of the analysis and close to the detection limit. The complete removal of chlorine-containing HCs, as reported by Bockhorn et al., could not be achieved with this setup (Bockhorn et al., 1998).

The analyses of the chemical composition support the findings deduced from elemental analyses. The comparison of the NMR results for the pyrolysis oils of different stages is shown in Fig. 7. The quantitative evaluation and the results of the isothermal reference experiment at 500 °C are shown in the supplementary information S3 according to the methodology of Netsch et al. (Netsch et al., 2026). Major differences

Table 3
Elemental composition of the condensate obtained from staged pyrolysis experiments and isothermal experiments at 500 °C with the STR Mix in the STR system.

Condensate	Elemental composition in wt.%					
	C	H	N	Cl	Moisture	O [A]
Isothermal 500 °C (Netsch et al., 2026)	84.4	12.5	0.6	0.5	0.0	2.0
Staged Pyrolysis						
400 °C (0 - 96 min)	60.7	11.7	1.3	7.0	15.0	4.8
500 °C (96 - 186 min)	85.6	13.7	0.2	0.2	0.0	0.3
Staged Pyrolysis						
430 °C (0 - 90 min)	82.8	11.7	1.0	1.7	1.7	1.0
500 °C (90 - 180 min)	86.8	12.6	0.3	0.2	0.0	0.0

[A] organic oxygen calculated as the difference to 100 wt.%.

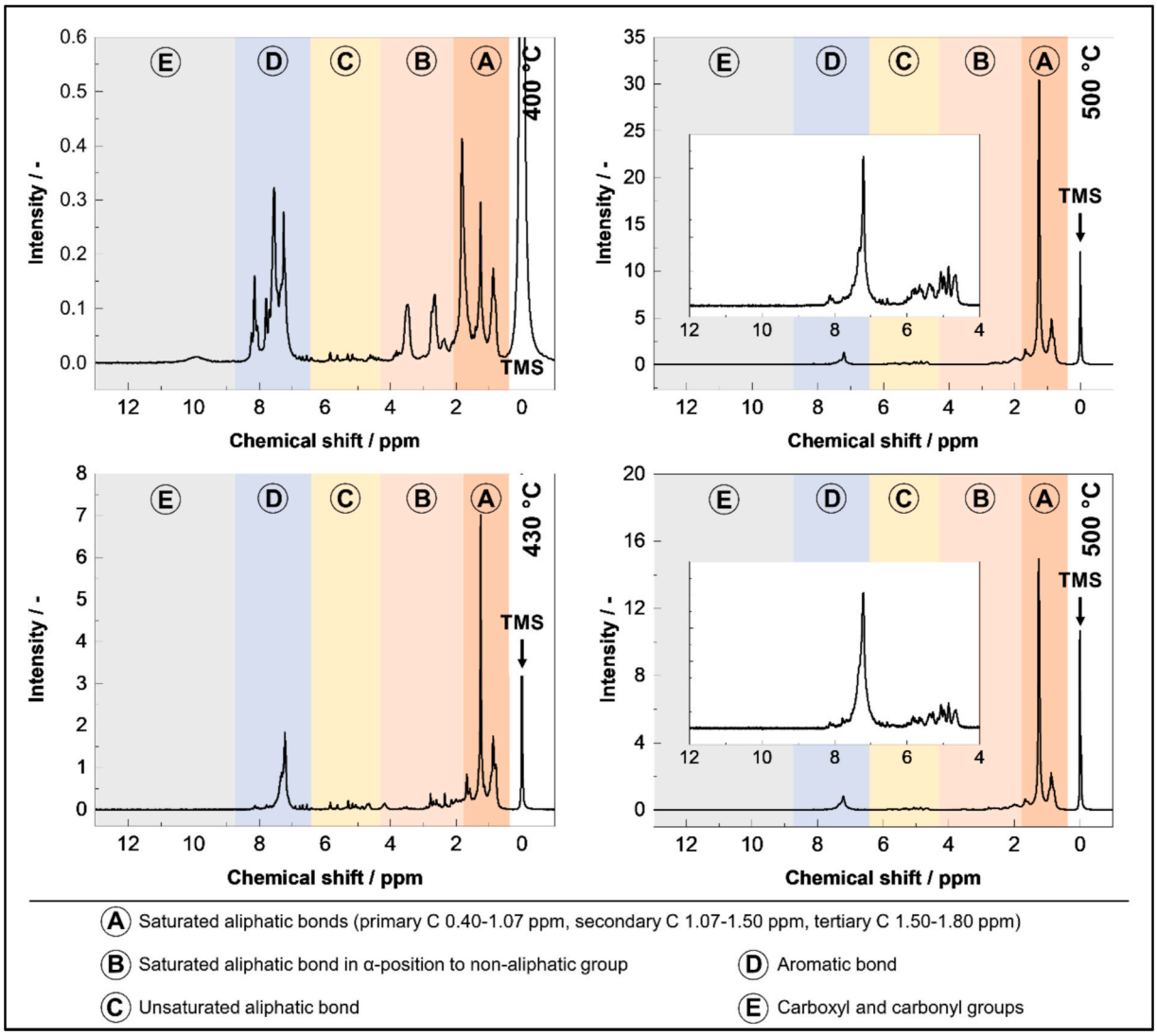

Fig. 7. NMR spectra of the pyrolysis oils obtained from the STR Mix pyrolyzed in two-staged experiments at temperature stages of 400 °C and 500 °C (top), and 430 °C and 500 °C (bottom). TMS indicates the chemical shift reference set to zero.

in the chemical composition of the condensate fractions are evident when comparing the first stage of the 400 °C experiment and the experiment at 430 °C. The condensate obtained in the first stage of the 400 °C test run requires dilution in deuterated chloroform. This preparation causes significantly lower signal intensities for this sample. Similar to the condensate of the 430 °C experiment, however, it exhibits more aromatic compounds and more protons close to a non-aliphatic functional group compared to the 430 °C product. The proportion of saturated aliphatic bonds is comparatively low. More aliphatic compounds are present in the 430 °C condensate than in the 400 °C condensate. This also reflects the higher carbon content determined in the elemental analysis for the 430 °C condensate compared to the 400 °C condensate. Consequently, the hypothesis of a substantial conversion of the polyolefinic components of the STR mix during the isothermal segment of the staged 430 °C pyrolysis is confirmed.

Carboxyl or carbonyl groups are detected in the 400 °C sample as a distinct peak at a chemical shift of 10 ppm. They reflect the high oxygen content indicated in the elemental analysis. Nevertheless, this peak is not visible in the 430 °C stage or the reference condensate obtained during the reference experiment under isothermal pyrolysis at 500 °C. The two condensate fractions collected in the second part of the staged pyrolysis are similar to each other but differ from the condensates produced in the respective experiment. Aromatic components are still present, but in lower proportions of 6.3 mol.% and 9.4 mol.%. The aliphatic-bound protons dominate with 80.8 and 77.0 mol.%. The ratio between saturated and unsaturated aliphatic-bound protons remains almost constant. No significant but only minor differences are detected via NMR between the oils of the respective 500 °C samples and the reference.

Additional GCxGC analyses were performed to quantify the shift of main HCs in both pyrolysis oils obtained during the 430 °C staged experiment. The condensate generated during the 400 °C experiment contains a high amount of water, preventing its analysis in the sensitive GCxGC system. The chromatograms indicate a complex composition of a multitude of different HC species. Different HCs that represent typical decomposition compounds of specific polymers serve as indicators to evaluate the separation of condensable species during the temperature-staged pyrolysis. 2,4-Dimethylheptene from PP, linear n-alkanes and α-olefins from PE, toluene as PS, ABS, and PET products, ε-caprolactam from PA6, and benzoic acid from PET are focused on. In the 430 °C stage, the condensate contains 1.7 wt.% of toluene, 1.0 wt.% of benzoic acid, and 1.1 wt.% of ε-caprolactam. These results exceed the concentrations found in the pyrolysis oil obtained after temperature increase (0.6 wt.%, 0.4 wt.%, and 0.5 wt.%, respectively). This emphasizes the predominant decomposition of the PS, ABS, PA6, and PET during the first stage, even though the elemental analysis does not reveal a distinct trend. Also, the

intensity of diphenyls and other monoaromatics is increased compared to the product generated at elevated pyrolysis temperatures of this test run. Consistent with the gas analyses, a partial degradation of PP is also verified by the GCxGC analyses. A concentration of 1.8 wt.% 2,4-Dimethylheptene is detected in the pyrolysis product at the 430 °C stage. The targeted product contains only 1.0 wt.% of 2,4-dimethylheptene, emphasizing the disadvantageous shift from PP products to the first stage. This shift might also be attributed to the PS-PP-specific interactions that were identified in TG. Nevertheless, the target product of the second pyrolysis stage includes a total amount of 13.6 wt.% of quantified n-alkanes and α-olefins in the range from C_7 to C_{20}. In the pyrolysis oil of the first stage, only 5.2 wt.% is detectable. This finding underlines the general feasibility of temperature staging to improve the quality of the pyrolysis oil and gas by depletion of heteroatom-containing compounds and aromatics.

In the STR system, the selective product enrichment by staged pyrolysis was less pronounced for the pyrolysis oil than for the gas. In particular, mass transport phenomena might cause this finding. While gases are quickly conveyed to the downstream sampling system by continuous nitrogen purging, condensable products must first perform a phase transition and drain into the collecting tanks. This represents an additional mass transport for condensable products and a potential source for artifact effects. The condensable products need more time to be collected than the flushing of pyrolysis gas. This causes a time delay for their collection, leading to a potential carryover of condensable products generated during the first stage to the oil collected at the elevated temperatures. Such a carryover of condensable product can be neglected for well-controlled laboratory-scale experiments. It poses a technical challenge in real plastic pyrolysis applications and might weaken the temperature stage separation effect in this study. This challenge might be overcome by a continuously operated cascade system of two reactors pyrolyzing at different temperatures. In such a cascade process, with each reactor having its own condensation unit, independence in the gas–liquid separation of the volatile products is achieved through spatial separation. Nevertheless, further investigation into the separation of pyrolysis oil and permanent gas in plastic pyrolysis condensation systems is generally necessary for the optimization of chemical recycling of plastics.

4. Conclusion

The results demonstrate the technical feasibility of the temperature-staged pyrolysis concept for selective product enrichment. Associated engineering challenges are also highlighted. TG experiments identified temperature ranges that enable partial separation of thermoplastics based on their distinct decomposition kinetics. However, interactions between polymers in mixed feedstocks can accelerate or delay their decomposition. For instance, interactions involving PVC, PA6, and PET accelerate low-temperature decomposition, while PS narrows the kinetic gap between low- and high-temperature stages by accelerating polyolefin decomposition. Although selective decomposition of aromatic and heteroatom-containing polymers around 370 °C is possible under TG conditions, partial conversion of polyolefins, particularly PP, cannot be fully avoided.

The staged pyrolysis concept was further validated in STR experiments. Compared to TG, stage temperatures and holding times must be adapted to account for heat and mass transfer limitations, batch operation, and time-dependent polymer temperature profiles. As a result, polymer temperatures remain below the reactor set temperature, requiring higher or prolonged operating conditions to achieve comparable separation effects. While variations in the first-stage temperature (400–430 °C) had little influence on the overall mass balance, they strongly affected the proportion of generated pyrolysis oil in each temperature stage. Higher first-stage temperatures enabled a pronounced reduction of heteroatoms and aromatics in the oil, as well as a targeted enrichment of aliphatic HCs in the oil obtained during the second stage.

The results demonstrate the key aspect of the optimization regarding the generation of an aliphatic-rich pyrolysis oil. Finding a balance between achieving maximum target product yield and improving the product quality is essential. Higher temperatures or longer holding times will cause complete decomposition of PS and ABS in the first isothermal stage. Polyolefins, especially PP, will pyrolyze more intensively. This would improve the oil quality but reduce the yield of the aliphatic-rich target product. On the contrary, the decomposition of polyolefins during the first pyrolysis stage is avoided by lower temperatures, but is also associated with a lower partial conversion of the non-polyolefinic thermoplastics. Establishing a clear priority between product yield and oil quality in plastic pyrolysis is only feasible to a limited extent. While industrial operation generally favors yield maximization due to its direct impact on revenues, heterogeneous and contaminated plastic waste streams inherently constrain yield improvements and necessitate subsequent oil upgrading. As upgrading efforts strongly depend on feedstock composition and process-specific conditions, a universal prioritization between yield and quality is not applicable. Consequently, defining a case-specific trade-off between yield and quality requires a dedicated techno-economic assessment, for which this work provides the relevant parameters.

The effective enrichment of heteroatom-containing gas species emphasizes the importance of appropriate process and equipment design during scale-up of staged pyrolysis processes. Corrosion, acidification, and clogging from accumulating salts like ammonium chloride are particularly related to HCl release. As a result, robust downstream pyrolysis gas cleaning and neutralization must be addressed, even if such effects were not observed at the pilot scale.

This study estimated the content of unsaturated aliphatics in the pyrolysis oil using NMR analyses. The results indicate that temperature-staged pyrolysis cannot significantly reduce its olefin content. Consequently, other process adjustments must be investigated to minimize the olefin content for pyrolysis oil application. Also, this study investigated well-defined feedstocks. This enables a detailed evaluation of the relationship between the decomposition of individual polymers and the overall yields and product composition. However, this selection limits the study, as other polymer types and impurities, such as biomass, may exhibit different reaction kinetics, which further influence the complex overall reaction mechanisms (Burra and Gupta, 2018; Zhao et al., 2025). Additionally, waste plastic products are typically highly functionalized. Incorporated additives influence pyrolysis kinetics through their decomposition behavior or possible interaction effects (Zhang et al., 2025; Charitopoulou et al., 2022). Consequently, the staged pyrolysis of representative waste fractions should also be investigated for optimization of staged pyrolysis systems.

Funding sources

The study was funded by the German Helmholtz Association within the program, “Materials and Technologies for the Energy Transition”.

CRediT authorship contribution statement

Niklas Netsch: Writing – original draft, Visualization, Validation, Methodology, Investigation, Formal analysis, Data curation, Conceptualization. **Aljoscha Tauber:** Investigation, Data curation. **Daniela Merz:** Writing – review & editing, Resources, Methodology, Conceptualization. **Britta Bergfeldt:** Resources, Formal analysis. **Salar Tavakkol:** Writing – review & editing, Supervision, Resources, Funding acquisition. **Dieter Stapf:** Writing – review & editing, Supervision, Resources, Funding acquisition.

Declaration of competing interest

The authors declare that they have no known competing financial interests or personal relationships that could have appeared to influence

the work reported in this paper.

Acknowledgment

-

Appendix A. Supplementary data

Supplementary data to this article can be found online at https://doi.org/10.1016/j.ces.2026.123622.

Data availability

Data will be made available on request.

References

Keijer, T., Bakker, V., Slootweg, J.C., 2019. Circular chemistry to enable a circular economy. Nat. Chem. 11, 190–195. https://doi.org/10.1038/s41557-019-0226-9.

van Geem, K.M., 2023. Plastic waste recycling is gaining momentum. Science 381, 607–608. https://doi.org/10.1126/science.adj2807.

European Parliament and the Council, Establishing the framework for achieving climate neutrality and amending Regulations (EC) No 401/2009 and (EU) 2018/1999 ("European Climate Law"), 2021.

Ragaert, K., Delva, L., van Geem, K., 2017. Mechanical and chemical recycling of solid plastic waste. Waste Manag. 69, 24–58. https://doi.org/10.1016/j.wasman.2017.07.044.

Johansen, M.R., Christensen, T.B., Ramos, T.M., Syberg, K., 2022. A review of the plastic value chain from a circular economy perspective. J. Environ. Manage. 302, 113975. https://doi.org/10.1016/j.jenvman.2021.113975.

Rahimi, A., García, J.M., 2017. Chemical recycling of waste plastics for new materials production. Nat. Rev. Chem. 1. https://doi.org/10.1038/s41570-017-0046.

Palos, R., Gutiérrez, A., Vela, F.J., Maña, J.A., Hita, I., Asueta, A., Arnaiz, S., Arandes, J. M., Bilbao, J., 2019. Assessing the potential of the recycled plastic slow pyrolysis for the production of streams attractive for refineries. J. Anal. Appl. Pyrol. 142, 104668. https://doi.org/10.1016/j.jaap.2019.104668.

Holtkamp, M., Renner, M., Matthiesen, K., Wald, M., Luinstra, G.A., Biessey, P., 2024. Robust downstream technologies in polystyrene waste pyrolysis: Design and prospective life-cycle assessment of pyrolysis oil reintegration pathways. Resour. Conserv. Recycl. 205, 107558. https://doi.org/10.1016/j.resconrec.2024.107558.

Laghezza, M., Fiore, S., Berruti, F., 2024. A review on the pyrolytic conversion of plastic waste into fuels and chemicals. J. Anal. Appl. Pyrol. 179, 106479. https://doi.org/10.1016/j.jaap.2024.106479.

Geyer, R., Jambeck, J.R., Law, K.L., 2017. Production, use, and fate of all plastics ever made. Sci. Adv. 3, e1700782. https://doi.org/10.1126/sciadv.1700782.

Bockhorn, H., Hornung, A., Hornung, U., Schawaller, D., 1999. Kinetic study on the thermal degradation of polypropylene and polyethylene. J. Anal. Appl. Pyrol. 48, 93–109. https://doi.org/10.1016/S0165-2370(98)00131-4.

Bockhorn, H., Hornung, A., Hornung, U., Weichmann, J., 1999. Kinetic study on the non-catalysed and catalysed degradation of polyamide 6 with isothermal and dynamic methods. Thermochim Acta 337, 97–110. https://doi.org/10.1016/S0040-6031(99)00151-3.

Faravelli, T., Pinciroli, M., Pisano, F., Bozzano, G., Dente, M., Ranzi, E., 2001. Thermal degradation of polystyrene. J. Anal. Appl. Pyrol. 60, 103–121. https://doi.org/10.1016/S0165-2370(00)00159-5.

Montaudo, G., Puglisi, C., Samperi, F., 1993. Primary thermal degradation mechanisms of PET and PBT. Polym. Degrad. Stab. 42, 13–28. https://doi.org/10.1016/0141-3910(93)90021-A.

Yu, J., Sun, L., Ma, C., Qiao, Y., Yao, H., 2016. Thermal degradation of PVC: a review. Waste Manag. 48, 300–314. https://doi.org/10.1016/j.wasman.2015.11.041.

Lee, K.-H., Shin, D.-H., Seo, Y.-H., 2006. Thermal degradation of nitrogen-containing polymers, acrylonitrile-butadiene-styrene and styrene-acrylonitrile. Korean J. Chem. Eng. 23, 224–229. https://doi.org/10.1007/BF02705720.

Kusenberg, M., Eschenbacher, A., Djokic, M.R., Zayoud, A., Ragaert, K., de Meester, S., van Geem, K.M., 2022. Opportunities and challenges for the application of post-consumer plastic waste pyrolysis oils as steam cracker feedstocks: to decontaminate or not to decontaminate? Waste Manag. 138, 83–115. https://doi.org/10.1016/j.wasman.2021.11.009.

Zhang, Y., Li, A., Zhang, Y.S., Xie, W., Liu, C., Peng, Y., Zhang, H., Kang, Y., Qu, B., Ji, G., 2024. In-situ catalytic pyrolysis of polyethylene to co-produce BTX aromatics and H2 by Ni/ZSM-5 in the rotary reactor with solid heat carriers. Fuel 371, 131950. https://doi.org/10.1016/j.fuel.2024.131950.

Cao, Y., Gao, R., Lei, J., Hou, Y., Xu, M., Cao, S., Chen, Z., Duan, Y., Du, H., 2025. Mechanistic insights into Cl transformation and calcium-based dechlorination during pyrolysis of waste plastics: Kinetics, product analysis and process optimization. J. Environ. Chem. Eng. 13, 119459. https://doi.org/10.1016/j.jece.2025.119459.

Kumar, A., Kumari, L., Laghari, A.A., Rong, H., Jamro, I.A., Sajnani, S., Aborisade, M.A., Rajput, G., Oba, B.T., Nkinahamira, F., Ndagijimana, P., Mehboob, G., Cui, B., Guo, D., 2024. Exploring the integrated potential of pyrolysis and low-temperature wet torrefaction for typical medical waste valorization: a multifaceted approach leveraging online TG-FTIR-MS, 2D-COS, iso-conversional kinetics, and reaction mechanisms. Chem. Eng. J. 499, 156464. https://doi.org/10.1016/j.cej.2024.156464.

Netsch, N., Schröder, L., Zeller, M., Neugber, I., Merz, D., Klein, C.O., Tavakkol, S., Stapf, D., 2025. Thermogravimetric study on thermal degradation kinetics and polymer interactions in mixed thermoplastics. J. Therm. Anal. Calorim. 150, 211–229. https://doi.org/10.1007/s10973-024-13630-6.

Bockhorn, H., Hornung, A., Hornung, U., 1998. Stepwise pyrolysis for raw material recovery from plastic waste. J. Anal. Appl. Pyrol. 46, 1–13. https://doi.org/10.1016/s0165-2370(98)00066-7.

Bockhorn, H., Hentschel, J., Hornung, A., Hornung, U., 1999. Environmental engineering: Stepwise pyrolysis of plastic waste. Chem. Eng. Sci. 54, 3043–3051. https://doi.org/10.1016/s0009-2509(98)00385-6.

Bockhorn, H., Hornung, A., Hornung, U., Jakobström, P., Kraus, M., 1999. Dehydrochlorination of plastic mixtures. J. Anal. Appl. Pyrol. 49, 97–106. https://doi.org/10.1016/S0165-2370(98)00124-7.

Faravelli, T., Bozzano, G., Colombo, M., Ranzi, E., Dente, M., 2003. Kinetic modeling of the thermal degradation of polyethylene and polystyrene mixtures. J. Anal. Appl. Pyrol. 70, 761–777. https://doi.org/10.1016/S0165-2370(03)00058-5.

Korkmaz, A., Yanik, J., Brebu, M., Vasile, C., 2009. Pyrolysis of the tetra pak. Waste Manag. 29, 761–777. https://doi.org/10.1016/S0165-2370(03)00058-5.

Cheung, W.Y., Lee, K.L., Lam, K.L., Chan, T.Y., Lee, C.W., Hui, C.-W., 2011. Operation strategy for multi-stage pyrolysis. J. Anal. Appl. Pyrol. 91, 165–182. https://doi.org/10.1016/j.jaap.2011.02.004.

Netsch, N., Tauber, A., Keskin, O., Bergfeldt, B., Wehner, H., Eidam, D., Tavakkol, S., Stapf, D., 2026. Chemical Recycling of Mixed Thermoplastics via Pyrolysis: A Comparative Study of Feedstock Influence and Reactor Impact. J. Anal. Appl. Pyrolysis 194, 107575. https://doi.org/10.1016/j.jaap.2025.107575.

Oyedun, A.O., Lam, K.L., Gebreegziabher, T., Hui, C.W., 2013. Optimization of multi-stage pyrolysis. Appl. Therm. Eng. 61, 123–127. https://doi.org/10.1016/j.applthermaleng.2013.03.043.

Choi, G.G., Oh, S.J., Kim, J.S., 2016. Non-catalytic pyrolysis of scrap tires using a newly developed two-stage pyrolyzer for the production of a pyrolysis oil with a low sulfur content. Appl. Energy 170, 140–147. https://doi.org/10.1016/j.apenergy.2016.02.119.

Oyedun, A.O., Lam, K.L., Hui, C.W., 2012. Charcoal Production via Multistage Pyrolysis. Chin. J. Chem. Eng. 20, 455–460. https://doi.org/10.1016/S1004-9541(11)60206-1.

Fukushima, M., Wu, B., Ibe, H., Wakai, K., Sugiyama, E., Abe, H., Kitagawa, K., Tsuruga, S., Shiruma, K., Ono, E., 2010. Study on dechlorination technology for municipal waste plastics containing polyvinyl chloride and polyethylene terephthalate. J. Mater. Cycles Waste Manage. 12, 108–122. https://doi.org/10.1007/s10163-010-0279-8.

López, A., de Marco, I., Caballero, B.M., Laresgoiti, M.F., Adrados, A., 2011. Dechlorination of fuels in pyrolysis of PVC containing plastic wastes. Fuel Process. Technol. 92, 253–260. https://doi.org/10.1016/j.fuproc.2010.05.008.

Lopez-Urionabarrenechea, A., de Marco, I., Caballero, B.M., Laresgoiti, M.F., Andrados, A., 2012. Catalytic stepwise pyrolysis of packaging plastic waste. J. Anal. Appl. Pyrol. 96, 54–62. https://doi.org/10.1016/j.jaap.2012.03.004.

Yuan, G., Chen, D., Yin, L., Wang, Z., Zhao, L., Wang, J.Y., 2014. High efficiency chlorine removal from polyvinyl chloride (PVC) pyrolysis with a gas-liquid fluidized bed reactor. Waste Manag. 34, 1045–1050. https://doi.org/10.1016/j.wasman.2013.08.021.

Yin, F., Zhuang, Q., Chang, T., Zhang, C., Sun, H., Sun, Q., Wang, C., Li, L., 2021. Study on pyrolysis characteristics and kinetics of mixed plastic waste. J. Mater. Cycles Waste Manage. 23, 1984–1994. https://doi.org/10.1007/s10163-021-01271-y.

Park, K.-B., Oh, S.-J., Guzelciftci, B., Kim, J.-S., 2018. Production of clean oil with low levels of chlorine and olefins in a continuous two-stage pyrolysis of a mixture of waste low-density polyethylene and polyvinyl chloride. Energy 157, 402–411. https://doi.org/10.1016/j.energy.2018.05.182.

Park, K.-B., Jeong, Y.-S., Guzelciftci, B., Kim, J.-S., 2019. Characteristics of a new type continuous two-stage pyrolysis of waste polyethylene. Energy 166, 343–351. https://doi.org/10.1016/j.energy.2018.10.078.

Park, K.-B., Choi, M.-J., Chae, D.-Y., Jung, J., Kim, J.-S., 2022. Separate two-step and continuous two-stage pyrolysis of a waste plastic mixture to produce a chlorine-depleted oil. Energy 244, 122583. https://doi.org/10.1016/j.energy.2021.122583.

N. Sophonrat, L. Sandström, I.N. Zaini, W. Yang, Stepwise pyrolysis of mixed plastics and paper for separation of oxygenated and hydrocarbon condensates, 229 (2018) 314-325. https://doi.org/10.1016/j.apenergy.2018.08.006.

Chang, T., Li, C., Fan, F., Wu, H., Wang, C., Yin, F., 2023. Effects of temperature zones on pyrolysis products of mixed plastic waste. J. Mater. Cycles Waste Manage. 25, 430–440. https://doi.org/10.1007/s10163-022-01549-9.

Williams, P.T., Williams, E.A., 1999. Interaction of Plastics in Mixed-Plastics Pyrolysis. Energy Fuels 13, 188–196. https://doi.org/10.1021/ef980163x.

PlasticsEurope, The Circular Economy for Plastics: A European Analysis, Brussels, 2024.

Netsch, N., Weigel, L., Schmedding, T., Zeller, M., Bergfeldt, B., Straczewski, G., Tavakkol, S., Stapf, D., 2025. Chemical Characterization of mixed plastic pyrolysis oils relevant for cracker reintegration by advanced two-dimensional gas chromatography. Fuel Process. Technol. 280, 108359. https://doi.org/10.1016/j.fuproc.2025.108359.

Cao, R., Zhang, M.-Q., Jiao, Y., Li, Y., Sun, B., Xiao, D., Wang, M., Ma, D., 2023. Co-upcycling of polyvinyl chloride and polyesters. Nat Sustain 6, 1685–1692. https://doi.org/10.1038/s41893-023-01234-1.

Jing, X., Zhao, Y., Wen, H., Xu, Z., 2013. Interactions between Low-Density Polyethylene (LDPE) and Polypropylene (PP) during the Mild Cracking of Polyolefin Mixtures in a Closed-batch Reactor. Energy Fuels 27, 5841–5851. https://doi.org/10.1021/ef401376m.

Westerhout, R.W.J., Waanders, J., Kuipers, J.A.M., van Swaaij, W.P.M., 1997. Kinetics of the Low-Temperature Pyrolysis of Polyethene, Polypropene, and Polystyrene Modeling, Experimental Determination, and Comparison with Literature Models and Data. Ind. Eng. Chem. Res. 36, 1955–1964. https://doi.org/10.1021/ie960501m.

Kruse, T.M., Levine, S.E., Wong, H.-W., Duoss, E., Lebovitz, A.H., Torkelson, J.M., Broadbelt, L.J., 2005. Binary mixture pyrolysis of polypropylene and polystyrene: a modeling and experimental study. J. Anal. Appl. Pyrol. 73, 342–354. https://doi.org/10.1016/j.jaap.2005.03.006.

Costa, P., Pinto, F., Ramos, A.M., Gulyurtlu, I., Cabrita, I., Bernardo, M.S., 2010. Study of the Pyrolysis Kinetics of a Mixture of Polyethylene, Polypropylene, and Polystyrene. Energy Fuels 24, 6239–6247. https://doi.org/10.1021/ef101010n.

Calero, M., Solís, R.R., Muñoz-Batista, M.J., Pérez, A., Blázquez, G., Ángeles Martín-Lara, M., 2023. Oil and gas production from the pyrolytic transformation of recycled plastic waste: an integral study by polymer families. Chem. Eng. Sci. 271, 118569. https://doi.org/10.1016/j.ces.2023.118569.

Chang, S.H., 2023. Plastic waste as pyrolysis feedstock for plastic oil production: a review. Sci. Total Environ. 877, 162719. https://doi.org/10.1016/j.scitotenv.2023.162719.

Maqsood, T., Dai, J., Zhang, Y., Guang, M., Li, B., 2021. Pyrolysis of plastic species: a review of resources and products. J. Anal. Appl. Pyrol. 159, 105295. https://doi.org/10.1016/j.jaap.2021.105295.

Burra, K.G., Gupta, A.K., 2018. Kinetics of synergistic effects in co-pyrolysis of biomass with plastic wastes. Appl. Energy 220, 408–418. https://doi.org/10.1016/j.apenergy.2018.03.117.

Zhao, N., Low, S.S., Law, C.L., Wu, T., Pang, C.H., 2025. Co-pyrolysis of polymers: recent advances, challenges and perspectives. Fuel Process. Tech. 274, 108239. https://doi.org/10.1016/j.fuproc.2025.108239.

Zhang, L., Zhou, N., Ke, L., Zeng, Y., Wu, Q., Zhang, J., Liao, R., Fan, L., Cobb, K., Ruan, R., Liu, Y., Wang, Y., 2025. Understanding the role of plastic additives in the pyrolysis of plastic wastes: Impact of additives on product selectivity, kinetics, and mechanistic pathways. Chem. Eng. J. 514, 163194. https://doi.org/10.1016/j.cej.2025.163194.

Charitopoulou, M.A., Papadopoulou, L., Achilias, D.S., 2022. Effect of brominated flame retardant on the pyrolysis products of polymers originating in WEEE. Environ. Sci. Pollut. Res. Int. 29, 29570–29582. https://doi.org/10.1007/s11356-021-15489-8.